Science of Remote Sensing 13 (2026) 100395

Contents lists available at ScienceDirect

Science of Remote Sensing

journal homepage: www.sciencedirect.com/journal/science-of-remote-sensing

Full length article

Improving national forest attribute maps of Sweden with machine learning

Dag Björnberg [a,b,*], Morgan Ericsson [b], Johan Lindeberg [c], Welf Löwe [a,b], Jonas Nordqvist [d], Jörgen Wallerman [e], Johan E.S. Fransson [c]

[a] Softwerk AB, Reveljgränd 5, 352 36 Växjö, Sweden
[b] Department of Computer Science and Media Technology, Linnæus University, Universitetsplatsen 1, 352 52 Växjö, Sweden
[c] Department of Forestry and Wood Technology, Linnæus University, Universitetsplatsen 1, 352 52 Växjö, Sweden
[d] Department of Mathematics, Linnæus University, Universitetsplatsen 1, 352 52 Växjö, Sweden
[e] Department of Forest Resource Management, Swedish University of Agricultural Sciences, Skogsmarksgränd 17, 901 83 Umeå, Sweden

ARTICLE INFO

Keywords:
Airborne laser scanning
Forest variable estimation
Forest mapping
Forest monitoring
Remote sensing

ABSTRACT

Remote sensing techniques are widely used for mapping and monitoring forest attributes, providing valuable information on forest cover, biomass, and overall forest health. In recent years, national airborne laser scanning (ALS) campaigns have been conducted in several countries to map forest resources. When combining ALS with field inventory data, these datasets enable the development of nationwide models for prediction of forest attributes. In this study, we explore the potential of machine learning (ML) to enhance existing modeling approaches for nationwide forest attribute mapping in Sweden. We achieve this by relating ALS data from the most recent ALS campaign of Sweden with field data from the Swedish National Forest Inventory (NFI). By aggregating laser metrics from surveyed areas (NFI plots), as well as over surrounding areas to the plots, we investigate (1) if ML approaches can outperform existing linear regression baseline models and (2) if further enhancements of the predictive capacity can be achieved by including surrounding, spatially correlated ALS data. To this end, we used extreme gradient boosting (XGBoost), as well as a convolutional neural network (CNN), specialized to handle tabular data and spatially correlated data, respectively. The models were evaluated on five forest variables: basal-area weighted mean tree height, basal-area weighted mean stem diameter, basal area, stem volume, and above-ground biomass. All models were evaluated on several nested datasets to assess the robustness, showcasing consistent results across datasets. We achieved significant improvements in prediction accuracy across all investigated forest variables. Furthermore, incorporating surrounding information to the modeling rendered further improvements for diameter, basal area, and biomass predictions. The approaches tested and developed here thus form a promising basis for flexible modeling approaches that can be transferred globally for large-scale forest monitoring and management.

1. Introduction

There is a need for better and more up-to-date forest mapping and monitoring to support decisions about the use of the forest as a national resource. This includes their role in providing raw materials for industry and energy, as well as storing carbon to benefit the climate. Forest owners also need improved tools and information to efficiently manage their forests. Consequently, several steps have been taken to automate the inventory process, which traditionally has been performed using sample-based field inventory data and manual interpretation of aerial images (Maltamo et al., 2021). More recently, airborne laser scanning (ALS) has been extensively applied to predict forest variables, for example in the Nordic countries (Næsset et al., 2004). In addition, national ALS campaigns along with field inventory data have made it possible to construct nationwide models for mapping of forest attributes, including examples from Finland (Maltamo et al., 2020) and Denmark (Nord-Larsen and Schumacher, 2012). These models enable the creation of high-resolution national raster databases covering key forest variables such as tree height and basal area. Improving these modeling approaches is crucial, not only for improving estimation accuracy, but also for supporting more detailed and effective forest management, often referred to as precision forestry (Dash et al., 2016).

The area-based approach summarizes ALS point clouds into statistical metrics for fixed areas (*e.g.* grid cells, plots, or stands), and links these metrics to field data to build predictive models for forest

* Corresponding author at: Department of Computer Science and Media Technology, Linnæus University, Universitetsplatsen 1, 352 52 Växjö, Sweden.
E-mail addresses: dag.bjornberg@lnu.se (D. Björnberg), morgan.ericsson@lnu.se (M. Ericsson), johan.lindeberg@lnu.se (J. Lindeberg), welf.lowe@lnu.se (W. Löwe), jonas.nordqvist@lnu.se (J. Nordqvist), jorgen.wallerman@slu.se (J. Wallerman), johan.fransson@lnu.se (J.E.S. Fransson).

https://doi.org/10.1016/j.srs.2026.100395
Received 26 May 2025; Received in revised form 5 February 2026; Accepted 10 February 2026
Available online 11 February 2026

attribute mapping at large scales (Næsset, 2002). This approach is the most commonly used for national forest attribute mapping and is well-suited due to its robustness and cost-efficiency. Moreover, national ALS campaigns are often performed using sparse point-cloud densities, making single-tree approaches less feasible.

Machine learning (ML) has been applied to various tasks, including the prediction of forest variables. In particular, area-based ML approaches have been investigated in several works. In Lee et al. (2018), support vector regression, modified regression trees, and random forests were used to estimate forest stand height. In Balazs et al. (2022), several ML approaches were compared when predicting growing stock, including k-nearest neighbors and variants of neural networks. ML approaches have also been tested relative to simpler linear regression techniques for modeling of the growing stock (Görgens et al., 2015; Parkitna et al., 2021).

The use of ML offers several advantages. An important benefit is that ML models often reduce or even eliminate the need for manual feature selection. Instead of relying on domain experts to hand-engineer which features matter most, many algorithms – especially deep learning and ensemble methods – can automatically discover relevant patterns and representations directly from the data (Bengio et al., 2013). Moreover, data-driven ML approaches can find intricate relationships between features and use these in combination to improve the model, even if they seem irrelevant in isolation (Domingos, 2012). Despite these advantages and the growing body of research, the use of ML for national forest monitoring and mapping remains limited.

Between 2009 and 2016, the Swedish national mapping, cadastral and land registration authority (Lantmäteriet) conducted the first nationwide laser scanning of Sweden with a resolution of 0.5–1 points per square meter. By relating metrics derived from ALS point-cloud data to sample plot measurements from the Swedish National Forest Inventory (NFI), candidate models were proposed to produce forest attribute maps over key forest variables (Nilsson et al., 2017). In particular, linear regression models for basal-area weighted mean tree height, basal-area weighted mean stem diameter, basal area, stem volume, and above-ground biomass were developed using ALS metrics extracted for each field plot together with inventory data. The Swedish Forest Agency made these maps available free of charge in a national raster database, featuring a $12.5\,\text{m} \times 12.5\,\text{m}$ grid cell size.

In 2018, a second nationwide ALS campaign over Sweden was launched, with a resolution of 1–2 points per square meter, further increasing the relevance of developing new methods for producing forest attribute maps. We investigate whether ML approaches can improve the prediction accuracy of the baseline linear regression models for the five forest variables. We focus on two ML approaches: extreme gradient boosting (XGBoost) applied to plot-level ALS metrics, and a convolutional neural network (CNN). XGBoost achieves state-of-the-art performance on tabular data tasks (Grinsztajn et al., 2022), making it a strong candidate for area-based ALS modeling. CNNs, in contrast, are well-suited for capturing spatial dependencies in raster-like data (Aggarwal, 2018). Therefore, we design a tailored CNN to test whether incorporating surrounding, spatially correlated information improves predictions. Although the degree of spatial autocorrelation may vary due to stand borders and heterogeneous surroundings, the nationwide character of the datasets can provide the CNN with sufficient variation to learn when surrounding information is useful and when it is not.

The predictive performance of the ML models and the baseline linear regression models was evaluated using data from the second nationwide ALS campaign. The models were assessed through repeated test splits, and a sensitivity analysis was performed to examine robustness under varying levels of potential outliers.

The objective of the study was to examine the potential of ML models for prediction of forest attributes at the national level in Sweden, and to suggest further improvements for the national forest attribute mappings. Additionally, a key focus was to develop a flexible ML approach that can be adapted for forest attribute prediction on a global scale. As a first step, the ML models used in this project will be transferred and evaluated for nationwide forest attribute prediction in Latvia. We believe that this work can inspire the forest research community to further investigate the advantages of these models at national levels.

2. Materials

2.1. NFI data

Since 1923, the Swedish NFI has been carried out using objective sample-based field inventory (Fridman et al., 2014). Inventory plots are located along the perimeters of rectangular areas known as tracts, with side lengths that decrease from north to south (1200 m in the north to 300 m in the south). The country is divided into five regions, with decreasing sampling intensity of tracts towards the north. The distance between tracts is large compared to the distance between plots within a tract (Ranneby et al., 1987). The number of plots within a tract depends on both the type of tract (permanent or temporary) and its geographic location.

Permanent tracts usually contain eight evenly distributed plots, although in the south this number is reduced to four. These tracts are revisited every fifth year and arranged in a systematic pattern according to the principles described in Ranneby et al. (1987). In contrast, temporary tracts are visited only once and placed randomly. Plot sizes also differ by tract type: permanent plots have a radius of 10 m, while temporary plots have a radius of 7 m. Overall, permanent plots account for about 60% of all NFI plots.

A wide range of forest variables are either measured or estimated for each plot. These include basal-area weighted mean tree height, basal-area weighted mean stem diameter, basal area, stem volume, and above ground biomass. All trees within the plots exceeding a threshold for the diameter at breast height (DBH) are calipered (for permanent plots this threshold is 4 cm whereas for temporary plots it is 10 cm). These DBH measurements are used to compute plot-level mean diameter and basal area. A random subsample of trees is selected and measured on height. Then a set of allometric regression models, described in Fridman et al. (2014), are used to obtain estimates of volume and biomass.

The plot coordinates were recorded with GPS receivers (Garmin GPSmap 60, 62, 64) with a horizontal accuracy of approximately 5 m (Persson et al., 2017).

2.2. ALS data

The second nationwide ALS campaign was initialized in 2018. The scanning is performed using a resolution of 1–2 points per square meter, a flying height of approximately 3 000 m, a scan angle of maximum 20°, a horizontal positional accuracy of 0.3 m, and a vertical positional accuracy of 0.1 m (on hard surfaces).

The scanning is carried out in blocks of approximately 25 km×50 km. To obtain a reliable representation of the ground surface, it is crucial that as many laser returns as possible reach the ground. During the vegetation season, however, leaves and undergrowth obstruct the laser pulses, reducing the number of ground returns. In southern Sweden, where broadleaved forests are common, this issue is particularly pronounced. Therefore, the ALS blocks in the south are scanned during the leaf-off season to ensure better ground coverage. The northern parts of Sweden are scanned primarily during the leaf-on season.

In total, 409 000 square kilometers of land is scanned. This encompasses all of Sweden, with the exception of certain mountainous areas in the north, where the forest cover is sparse (forest land less than 10% within a 2.5 km grid). These areas are excluded from the scanning.

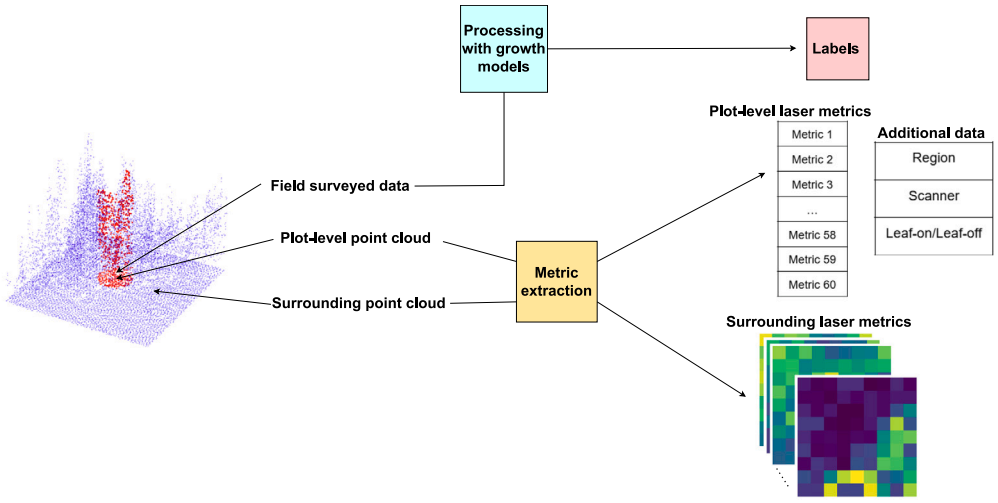

Fig. 1. Data processing. ALS point clouds were collected over 90 m × 90 m areas centered on NFI plots. Plot-level ALS metrics were computed by clipping the point cloud to the extent of each plot, while surrounding-area ALS metrics were calculated across the full 90 m × 90 m area using 10 m × 10 m grid cells. In both cases, 60 ALS metrics were computed. Additional inputs included region, scanner type, and leaf-on/leaf-off condition. The field data (used as labels) were adjusted with allometric growth models to match the date of scanning.

3. Methods

This section describes the data processing, modeling, and evaluation steps used in the study. We start by describing the ALS metrics, followed by the selection and temporal alignment of NFI plot data. These inputs are then used to calibrate the baseline linear regression and ML models. An overview of the full workflow for the data processing is provided in Fig. 1.

3.1. ALS metrics

The ALS data used in this study were collected between May 2018 and May 2023. The ALS point-cloud data were processed using the lidR package (Roussel et al., 2020). For each NFI plot, the point cloud was clipped to the plot boundary, and plot-level ALS metrics were derived.

To also capture spatial context, we computed metrics from a 90 m × 90 m window centered on each plot. By design (see Section 2.1), these windows do not overlap between plots. This setup provides information on the surrounding forest structure while also preventing data leakage between plots. Within each window, ALS metrics were derived from a grid of 10 m × 10 m cells.

The raw point-cloud data were normalized using the lidR function `normalize_height()` with the knnidw algorithm, an inverse distance weighting approach with k-nearest neighbors (Janiec et al., 2025). Plot-level metrics were computed using `cloud_metrics()`, while grid-level metrics (from 10 m × 10 m cells within each 90 m × 90 m window) were computed using `pixel_metrics()`. Both functions can accept either custom metric functions or predefined sets of standardized ALS metrics. We used the predefined set of metrics provided by `stdmetrics()`. Additionally, we added the first four L-moments, because these have been shown valuable in ALS-based modeling studies (Valbuena et al., 2017).

In total, 60 metrics were used, shown in Table 1. The metrics are primarily height metrics and intensity metrics. The intensity metrics were not calibrated between flights, which may yield noisy intensity values. However, raw intensity has been used in nationwide forest inventory applications, such as in Denmark (Nord-Larsen and Schumacher, 2012). In general, we did not conduct a study to select a subset of useful metrics to be used for the ML approaches. Although adding non-informative metrics may introduce noise in the model fitting process, the relationships between different metrics are often intricate, and it can be difficult to determine their relevance *a priori*. Consequently, we use different regularization techniques (see Section 3.4) to minimize the risk of overfitting issues.

Table 1
Description of the 60 ALS metrics used in the study.

Notation	Explanation
$z_{\max}$, z_{mean}, z_{sd}, z_{skew}, z_{kurt}, z_{entropy}	Height maximum, mean, standard deviation, skewness, kurtosis, and entropy
z_{qx}, $x = 5, 10, 15, \ldots, 90, 95$	Height percentiles
$p_{\text{zabovezmean}}$, p_{zabove2}	Proportion of all returns above z_{mean} and above 2 m
z_{pcumx}, $x = 1, 2, 3, \ldots, 9$	Cumulative percentage of all returns in lower $10 \cdot x$% of $z_{\max}$
i_{tot}	Sum of intensities for each return
$i_{\max}$, i_{mean}, i_{sd}, i_{skew}, i_{kurt}	Intensity maximum, mean, standard deviation, skewness, and kurtosis
i_{pground}	Percentage of intensity returned by points classified as ground
i_{pcumzqx}, $x = 10, 30, 50, 70, 90$	Percentage of intensity returned below the xth percentile of height
p_{xth}, $x = 1, 2, 3, 4, 5$	Percentage of xth return
p_{ground}	Percentage of all returns classified as ground
n	Number of returns
$area$	Approximate area of raster
L_1, L_2, L_3, L_4	L-moments

We also included categorical data for scanner type (to account for the two different scanners that were used), leaf-off/leaf-on condition, and the Swedish regions: Götaland, Svealand, southern Norrland, and northern Norrland. These were included in all of our models either as dummy variables (for the linear regression models) or as direct inputs (for the ML approaches).

3.2. NFI plot data selection and temporal alignment

For our purposes, a total of 18 218 NFI plots, field surveyed between April 2018 and November 2022 were considered. Permanent plots are less sensitive to positional errors compared to temporary plots due to the larger plot area (10 m radius compared to 7 m radius). Hence, we decided to include only permanent plots in our investigation, of which there were 10 084. The permanent plot locations are displayed in Fig. 2.

Due to thinning and felling operations, the dataset contains a number of plots where the ALS data clearly cannot be related to the NFI data. Such plots were identified by building a linear regression

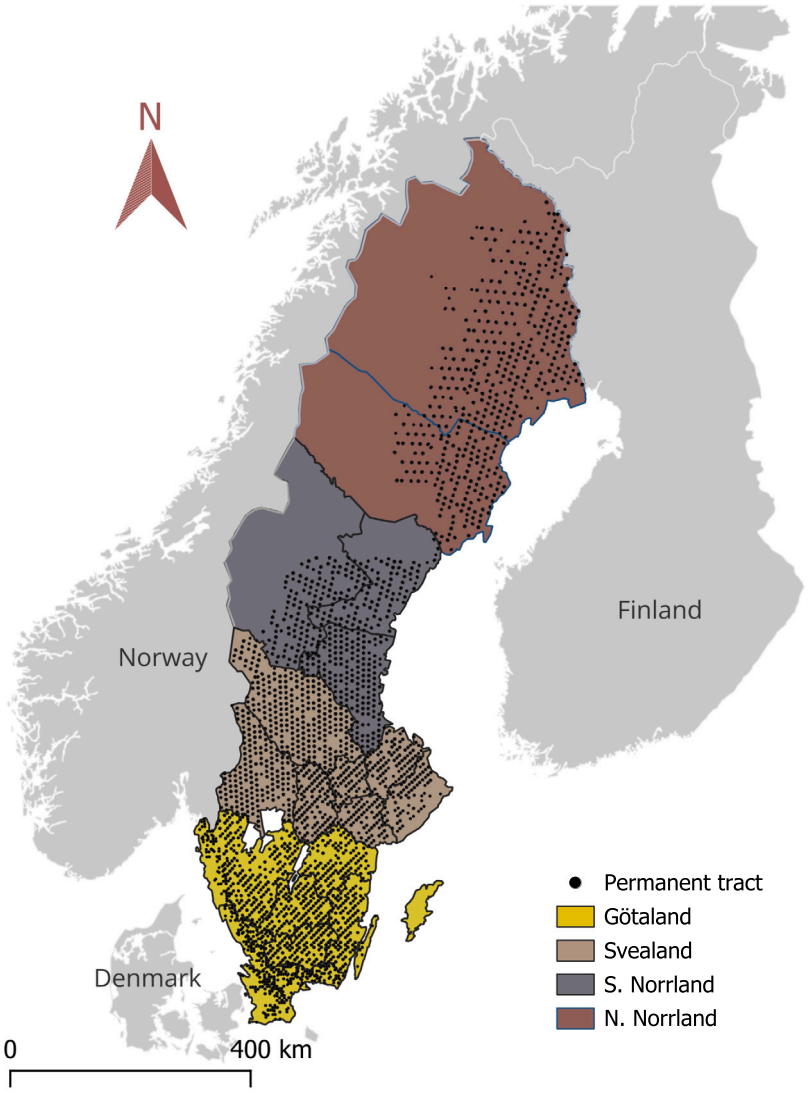

Fig. 2. Map over Swedish regions along with permanent NFI tract locations considered in our investigation.

height model using the 95th plot-level height percentile as explanatory variable, and field-measured tree height as response variable. Datapoints deviating from the fitted regression line by more than ±4.8 m were removed. This threshold was chosen based on the annual average harvested stem volume in Sweden, which corresponds to approximately 3.6% (Eliasson et al., 2019). In other words, the cutoff was set such that roughly 3.6% of the dataset was excluded. Although this pruning strategy is not perfect, it is grounded in national forest harvesting statistics and removes a reasonable proportion of the data likely to be affected by harvesting-related activities. In particular, it helps eliminate obvious mismatches between field data and ALS measurements caused by felling operations. Similar pruning strategies were used in Maltamo et al. (2020) and Nilsson et al. (2017). This pruning procedure is illustrated in Fig. 3. After this cleaning step, 9 721 permanent plots remained. Table 2 summarizes the field data for the retained plots.

To account for the time difference between the date of the field measures and the laser scanning, the NFI data were either backcasted or forecasted with allometric growth models using the Heureka Forestry Decision Support System (Elfving and Nyström, 2010). The Heureka system is commonly used in Sweden for forecasting forest variables. The models are developed based on NFI data and have shown to give reliable growth estimates (Nilsson et al., 2017; Fahlvik et al., 2014).

3.3. Linear regression models

Baseline linear regression models were calibrated using plot-level ALS metrics and NFI data. In previous work (Nilsson et al., 2017), separate local regression models were fitted for each ALS block of Sweden, each containing approximately 350 NFI plots. In contrast, our approach does not reuse those block-specific models. Instead, we calibrated new nationwide regression models using the full dataset.

To make a single set of models applicable across all of Sweden, we incorporated additional dummy variables for region (to distinguish between four regions), scanner type (to account for the two different scanners that were used), and leaf-on/leaf-off condition. These terms allow the nationwide models to account for regional and situational variability that was previously captured implicitly by localized model fitting. In this way, we obtain baseline models that are directly comparable to the unified ML models evaluated in this study.

The final regression models are presented in Table 3. Parameter estimation was performed using the `ols()` function from the statsmodels library in Python (Seabold et al., 2010).

3.4. ML approaches

We used two ML approaches. In the first approach, we applied extreme gradient boosting (XGBoost) (Chen and Guestrin, 2016), an

Table 2
Statistics over the NFI plot attributes used in the study.

	Height (m)		Diameter (cm)		Basal area (m^2/ha)		Volume (m^3/ha)		Biomass (ton/ha)		No. of plots
	Mean	Range	Mean	Range	Mean	Range	Mean	Range	Mean	Range	
Götaland	16	0–34	21	0–100	23	0–78	193	0–1075	102	0–484	3104
Svealand	14	0–33	19	0–58	21	0–67	172	0–792	91	0–362	3019
S. Norrland	13	0–29	17	0–75	20	0–67	151	0–790	81	0–327	1739
N. Norrland	11	0–26	16	0–40	17	0–58	112	0–611	63	0–295	1859
Entire Sweden	14	0–34	19	0–100	21	0–78	164	0–1075	87	0–484	9721

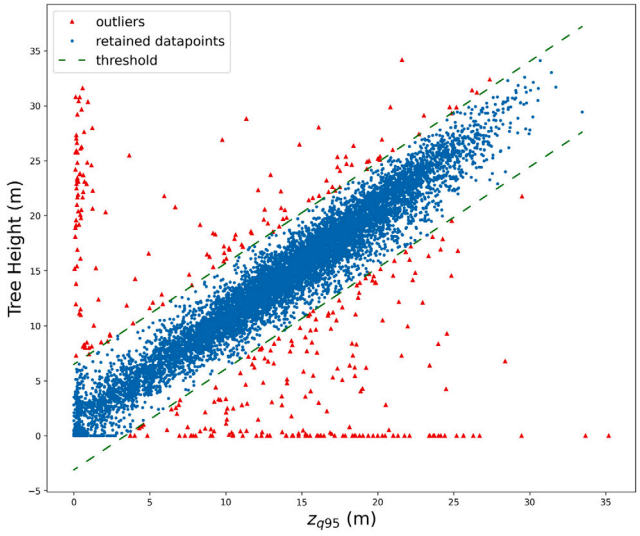

Fig. 3. Data pruning strategy. Plots likely affected by felling or thinning operations were identified by fitting a linear regression model using the 95th-percentile plot-level ALS height (z_{q95}) as the explanatory variable and plot tree height as the response variable. Observations deviating from the regression line by more than ±4.8 m were excluded. This threshold was chosen so that the proportion of removed observations matched the yearly harvested stem volume, which is approximately 3.6%.

ensemble method based on decision trees. In the second approach, we tested whether including a surrounding area would be beneficial for improving the predictions. This was achieved using a CNN. Both ML approaches were trained using a train/validation split, where the validation set was used for early stopping and model selection.

3.4.1. XGBoost

Gradient boosting, described in Friedman (2001), iteratively fits a simple parameterized function (base learner) to the current data-based gradient (pseudo-residuals). The model can then be updated using steepest-descent at every iteration. This process is repeated until a stopping criterion is met, and the final model F is an additive expansion of all fitted base learners: $F(\mathbf{x}) = \sum_m \beta_m h(\mathbf{x}; \mathbf{a}_m)$, where $h(\mathbf{x}; \mathbf{a}_m)$ is the base learner (typically a decision tree), and β_m is a parameter found via line search, determining the optimal step size.

Extreme gradient boosting (XGBoost) builds on the gradient boosting paradigm. The base learner is a decision tree with a predefined maximum depth. It also introduces regularization in the objective function and incorporates second-order derivatives to improve optimization (Chen and Guestrin, 2016). XGBoost has shown state-of-the-art performance for tabular data tasks, generally outperforming deep learning models in these scenarios (Grinsztajn et al., 2022). It has also shown impressive performance in several remote sensing applications (Zamani Joharestani et al., 2019; Vijaywargiya and Ramiya, 2024). See Fig. 4 for a schematic overview of XGBoost.

We used a maximum depth of 3; increasing this hyperparameter value above this threshold did not further enhance the predictive capacity of the models. A maximum ensemble size of 1000 trees was used, and we applied an early stopping on the validation set after five iterations, *i.e.*, if the predictions were not improved over the last five added decision trees, the model fitting was interrupted and the model with the best performance on the validation set was chosen to compute the predictions on the test set. In total, all 60 plot-level ALS metrics were used, along with data for region, scanner type, and leaf-on/leaf-off condition.

Table 3
The baseline linear regression models that were used to predict the five forest attributes. Note that dummy variables for region, scanner type, and leaf-on/leaf-off condition are included in the models, but are not explicitly shown.

Variable	Linear regression models[a]
Height (m)	$hbw_1 = \beta_0 + \beta_1 z_{q95}$
Diameter (cm)	$dbw_1 = \beta_0 + \beta_1 z_{q80} + \beta_2 (z_{q80} \cdot p_{\text{zabove2}})$ $dbw_2 = \beta_0 + \beta_1 z_{q90} + \beta_2 (z_{q90} \cdot p_{\text{zabove2}})$ $dbw_3 = \beta_0 + \beta_1 z_{q80} + \beta_2 (z_{q90} \cdot p_{\text{zabove2}})$ $dbw_4 = \beta_0 + \beta_1 z_{q90} + \beta_2 (z_{q80} \cdot p_{\text{zabove2}})$
Basal area (m^2/ha)	$ba_1 = \beta_0 + \beta_1 (z_{q80} \cdot p_{\text{zabove2}}) + \beta_2 z_{\text{sd}}$ $ba_2 = \beta_0 + \beta_1 (z_{q90} \cdot p_{\text{zabove2}}) + \beta_2 z_{\text{sd}}$
Volume (m^3/ha)	$\sqrt{v}_1 = \beta_0 + \beta_1 z_{q80} + \beta_2 (z_{q80} \cdot p_{\text{zabove2}}) + \beta_3 z_{\text{sd}}$ $\sqrt{v}_2 = \beta_0 + \beta_1 z_{q90} + \beta_2 (z_{q90} \cdot p_{\text{zabove2}}) + \beta_3 z_{\text{sd}}$ $\sqrt{v}_3 = \beta_0 + \beta_1 z_{q80} + \beta_2 (z_{q90} \cdot p_{\text{zabove2}}) + \beta_3 z_{\text{sd}}$ $\sqrt{v}_4 = \beta_0 + \beta_1 z_{q90} + \beta_2 (z_{q80} \cdot p_{\text{zabove2}}) + \beta_3 z_{\text{sd}}$
Biomass (ton/ha)	$\sqrt{bio}_1 = \beta_0 + \beta_1 z_{q80} + \beta_2 p_{\text{zabove2}} + \beta_3 z_{\text{sd}}$ $\sqrt{bio}_2 = \beta_0 + \beta_1 z_{q90} + \beta_2 p_{\text{zabove2}} + \beta_3 z_{\text{sd}}$

[a] z_{qx} = height percentile, p_{zabove2} = percentage of returns above 2 m, and z_{sd} = standard deviation of height distribution.

3.4.2. CNN

A CNN is a deep learning approach, specialized in handling spatially correlated data, such as images (Aggarwal, 2018). It consists of learnable weights (parameters) and optimizes these weights by minimizing a loss function, using gradient-based optimization. The key components of a CNN architecture are the following:

- *Convolution*: Uses a sliding window (kernel) that convolves the data with learnable weights, to detect different features like edges or patterns.
- *Pooling*: Aims to reduce the output size of a feature map. Can involve max-pooling (summarizing all values in a grid by the maximum), or average pooling (summarizing with average value). The pooling operation makes the network more invariant to small distortions in the input.
- *Fully connected layers*: Typically applied after convolution layers and pooling layers, to learn complex relationships between extracted features.
- *Activation function*: Nonlinear function applied to enforce the network to handle complex relationships within data. The most common activation function is the rectified linear unit (ReLU) defined by $\text{ReLU}(x) = \max(0, x)$.

CNNs have been extensively applied to various forestry and agricultural remote sensing tasks (Kattenborn et al., 2021), where spatial

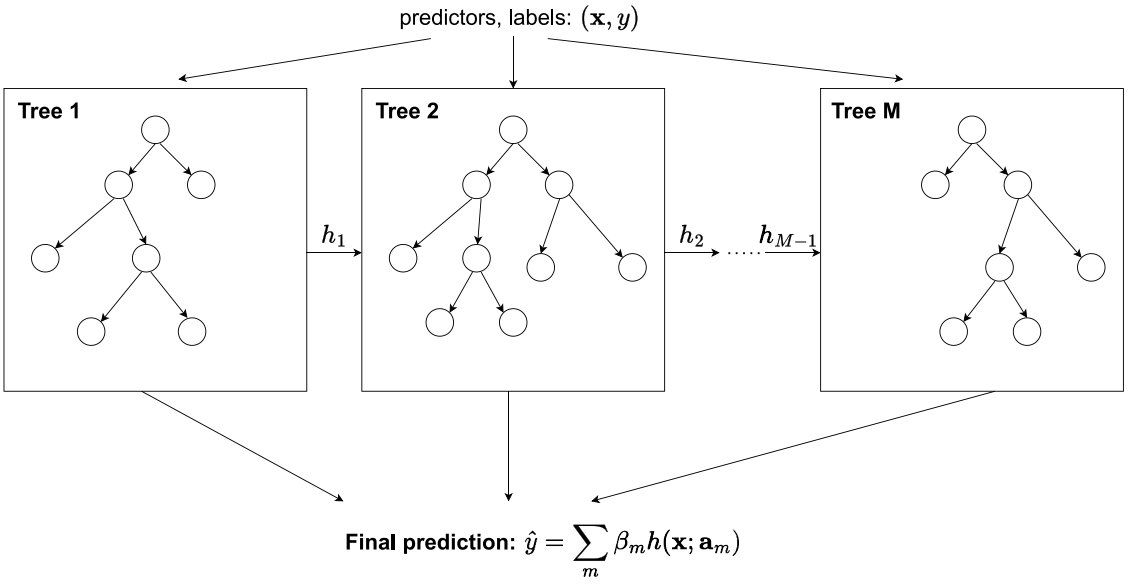

Fig. 4. General scheme for XGBoost. A series of regression trees are fitted on the predictors and corresponding labels. In our case the predictors are represented by 60 ALS metrics along with region, scanner type and leaf-on/leaf-off condition, whereas the labels are measurements from the NFI plots. Each tree's residuals are used for fitting the next tree. The final prediction is an additive expansion of all fitted trees.

vegetation patterns are present. The existence of spatial autocorrelation among forest attributes is supported by several studies, such as Tuominen et al. (2017) and Zhang et al. (2023). Even if the plot characteristics do not necessarily reflect its surroundings, with a sufficiently large training dataset, a CNN can learn to differentiate cases where nearby areas are consistent with the plot and contribute with useful information, versus cases where they differ and should be down-weighted in the prediction.

To incorporate surrounding ALS data, we use a CNN on surrounding raster data. The convolutional layers process this "grid of metrics" and extracts a feature map. This output feature map is then concatenated with plot-level ALS metrics. The final prediction is made by passing this combined input through fully connected layers. In this way, we utilize both the explicit plot-level ALS metrics, as well as surrounding information. The proposed architecture is outlined in Fig. 5. The surrounding raster data was a $90\,\text{m} \times 90\,\text{m}$ square, where the ALS metrics were aggregated in $10\,\text{m} \times 10\,\text{m}$ grid cells, resulting in a 9×9 pixel image with 60 channels. Although these derived metrics may not be optimal for use with a CNN, this approach provides an effective and computationally tractable way to summarize the surrounding data for use with a 2D-CNN.

To improve training stability and prevent overfitting, a number of regularization techniques were employed, such as inclusion of dropout (Baldi and Sadowski, 2013), a learning rate scheduler (Wen et al., 2021), and early stopping after 10 consecutive non-improving iterations on the validation loss. Additionally, we performed augmentations on the surrounding raster images in the form of rotations and mirroring during training to artificially expand the training dataset.

3.5. Sensitivity analysis

In Section 3.2, plots likely to be affected by harvesting-related activities were removed. However, other types of outliers and anomalies may still remain due to various factors. In Knott et al. (2023), four primary types of outliers arising from geospatial data harmonization were identified:

1. *Procedural outliers*: Deviations caused by inconsistencies or limitations in the NFI protocol, such as changes in measurement definitions, or errors during manual data recording.
2. *Spatial mismatches*: Occur when recorded GNSS coordinates of NFI plots or the remotely sensed data accuracy are imprecise, leading to a misalignment between the field plot and the corresponding remote sensing data.
3. *Temporal mismatches*: Arise from differences in the timing of data collection between remotely sensed data and field measurements. Field attributes may change during this interval (e.g., due to harvesting or wind damages).
4. *Statistical outliers*: Datapoints that deviate significantly from the majority of the data distribution, often caused by rare but valid conditions such as the presence of exceptionally large trees.

In the case of Sweden, the NFI protocol for estimating the forest variables has remained intact since 2003 (Fridman et al., 2014). Consequently, we expect that the outliers available in our dataset mainly belong to categories 2–4. The question of how to deal with these outliers is not trivial. Removing none or too few of the datapoints may result in a dataset with many obvious errors, skewing the predictions and prohibiting the modeling approaches from learning accurately. Being too aggressive in the outlier removal brings into question whether the remaining dataset can still be viewed as a probability sample from the NFI. Given the large size and complexity of the dataset, manual inspection is infeasible to remove such outliers.

A robust statistical approach to reduce outliers is to use the Mahalanobis distance (De Maesschalck et al., 2000), which accounts for the correlations between features in a multivariate space. We constructed a five-dimensional feature space spanned by the residuals of predicted versus actual values. The residuals were computed using the first indexed baseline linear regression models in Table 3 (hbw_1, dbw_1, ba_1, $\sqrt{v_1}$, and $\sqrt{bio_1}$). Although this method does not explicitly model the four types of outliers, it provides a mechanism to identify datapoints that deviate substantially from the joint feature distribution. Such points are more likely to correspond (directly or indirectly) to one or more of the identified outlier categories. A similar mechanism for outlier reduction was employed in de Lera Garrido et al. (2023),

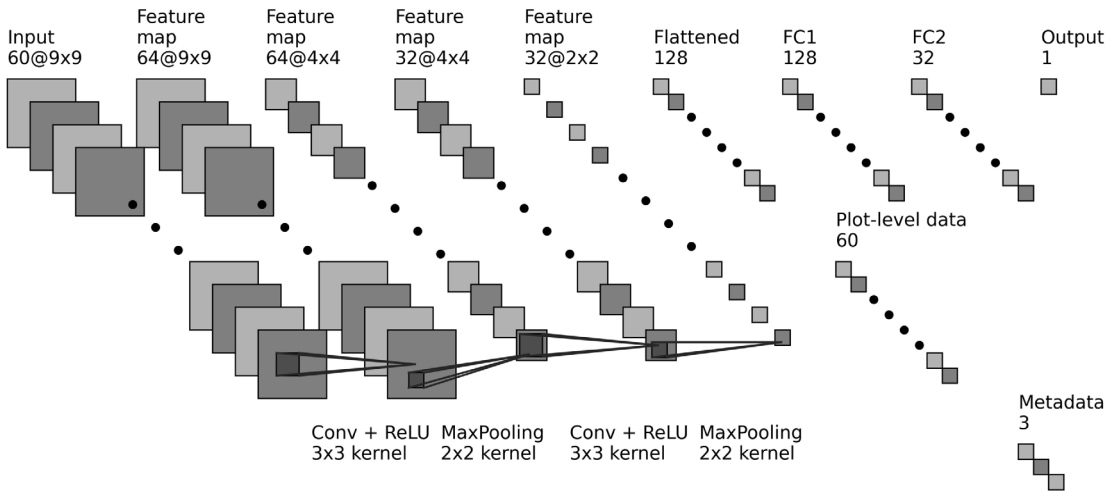

Fig. 5. Proposed architecture for the CNN. Raster data surrounding the NFI plot, aggregated into a 9 × 9 pixel image is processed by the CNN to construct a feature map. The feature map is then concatenated with plot-level ALS metrics, along with data for region, scanner type and leaf-on/leaf-off condition. The final output is obtained by further processing with fully connected layers.

where Rosner's test (Rosner, 1983) was used to automatically detect outliers. To assess the robustness of our approaches and to explore the effects of varying degrees of outlier filtering, we progressively removed 0% (original), 5%, 10%, 15%, and 20% outlier datapoints from the previously processed dataset (i.e., after the initial 3.6% removal based on harvesting statistics). The 20% threshold was chosen arbitrarily by the authors as a reasonable upper bound.

The goal of this sensitivity analysis was not to determine the optimal number of outliers to remove, but to assess the robustness of the models relative to different levels of potential outliers. The datapoints identified and removed through this procedure are not confirmed errors, but rather observations that are statistically distant in the joint feature space, given a specified threshold. Consequently, observed changes in RMSE should be interpreted as a byproduct of data filtering rather than as an indication of improved generalization.

3.6. Model evaluation

We adopted a bootstrap methodology with randomly selected test sets covering the whole of Sweden. In each experiment, 5% of the data was included in the test set, and the remaining 95% was used for model calibration. For the ML approaches, 15% of the calibration data was set aside for validation and used together with an early stopping criterion to prevent overfitting. The remaining data was used for training. The linear regression models were fitted using the entire calibration dataset.

For the baseline linear regression models, the variant with the lowest test RMSE was selected to represent the results for each experiment. This may yield slightly optimistic RMSE estimates for the linear regression models, since the test data were also used for model selection. In contrast, the ML approaches were selected on the basis of an independent validation set, so their test RMSE estimates remain unbiased.

To obtain reliable estimates, the random 5% test selection was repeated 50 times. For each experiment, the models were recalibrated using the remaining 95% of the data. As the datasets are nationwide (hence covering nationwide conditions), no independent validation was performed at the stand level. A schematic overview of the evaluation methodology is provided in Fig. 6. This evaluation methodology was used in all our experiments, both for the pruned dataset described in Section 3.2, and for the sensitivity analysis (Section 3.5).

To validate our results, we performed statistical tests using both the paired t-test and the Wilcoxon signed-rank test. These tests compared RMSE values for each method across all five datasets used in the sensitivity analysis. As a total of 50 experiments were conducted across each of the five datasets, a total number of 250 RMSE values were compared. Statistical significance was assessed between (i) the baseline and the best-performing ML approach, and (ii) XGBoost and CNN. This allowed us to evaluate two key aspects: (1) whether our ML approaches outperform the baseline methods, and (2) if leveraging a CNN, and thus including surrounding information, provides an advantage over using only plot-level data.

4. Results

4.1. Model performance after harvesting-related pruning

The results reported here are based on the dataset processed according to the strategy described in Section 3.2. The results showed that the use of ML models improved the results compared to the baseline linear regression models (see Fig. 7). There were also indications that including a surrounding area and employing a CNN modeling approach further enhanced the predictions of diameter, basal area, and biomass. In other words, the CNN produced a lower RMSE compared to XGBoost on these three attributes, where RMSE was reduced by 1.7% for diameter, 3.0% for basal area, and 2.7% for biomass (on average). For tree height, XGBoost gave the best predictions, whereas CNN produced results more similar to those of the linear regression model. For volume predictions, we did not see any additional benefits when incorporating a surrounding area, as CNN and XGBoost produced similar results.

For all attributes, a clear trend can be observed with a decrease in RMSE from south to north, reflecting the generally smaller tree sizes in the northern regions, where colder temperatures and reduced sunlight limit growth. This trend is also evident in Table 2, and visually represented in Fig. 8. Furthermore, more heterogeneous forests in southern Sweden, in terms of tree species composition, tree size, and spatial distribution, could theoretically, to some extent, explain the higher RMSE estimates in the southern parts of Sweden. However, this hypothesis is not clearly supported by the relative RMSE estimates, as shown in Fig. 9.

4.2. Sensitivity analysis

The sensitivity analysis showed consistent results across all filtered datasets, indicating that the ML models are robust to different levels of potential outliers, as identified via the progressive filtering procedure described in Section 3.5. For diameter, basal area, and biomass, we

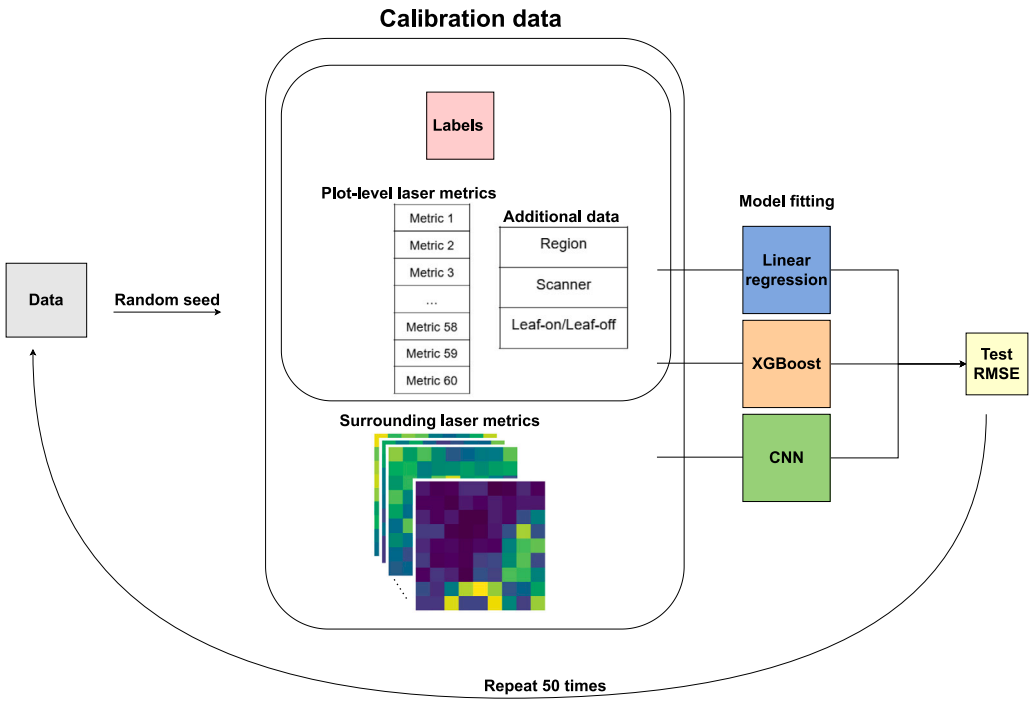

Fig. 6. Evaluation methodology used in the experiments. The dataset was randomly split into a calibration set (95%) and a test set (5%). For the ML approaches, 15% of the calibration set was used for validation. The approaches were evaluated on the test set, and this process was repeated 50 times. The baseline linear regression models and XGBoost used plot-level ALS metrics, whereas the CNN incorporated even surrounding ALS metrics.

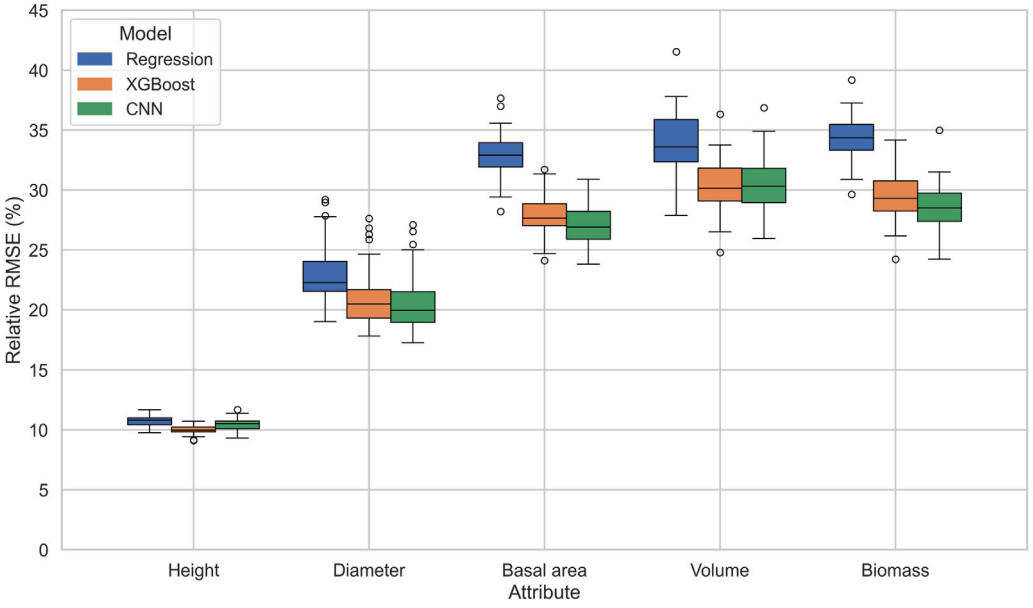

Fig. 7. Boxplots summarizing RMSE values across 50 experiments for forest attribute predictions over Sweden using different modeling approaches.

observe an improvement by including surrounding information and leveraging a CNN. The differences are small compared to the results obtained with XGBoost, 0.0%−1.7% for diameter, 1.6%−3.0% for basal area, and 0.4%−2.7% for biomass. The results are visualized in Fig. 10.

Despite the small differences, the consistency across datasets suggests that the surrounding information possesses meaningful predictive capacity, at least for those specific attributes. This hypothesis was further supported by the paired t-test and the Wilcoxon signed-rank test, comparing RMSE values over all 250 experiments (RMSE values from all five datasets combined). Both tests demonstrated clear statistical significance (p-value $\ll 0.05$). In the same way, these statistical tests were performed to compare the baseline linear regression models with the best ML approach for each respective variable, with clear statistical significance in all cases. The significance results are shown in Table 4.

5. Discussion

This study aimed to test whether area-based ML techniques can be used to improve forest attribute maps of Sweden compared to baseline linear regression techniques that have previously been used. To this end, we considered two ML approaches: XGBoost and a customized CNN. Both methods were used to assess if ML can enhance forest

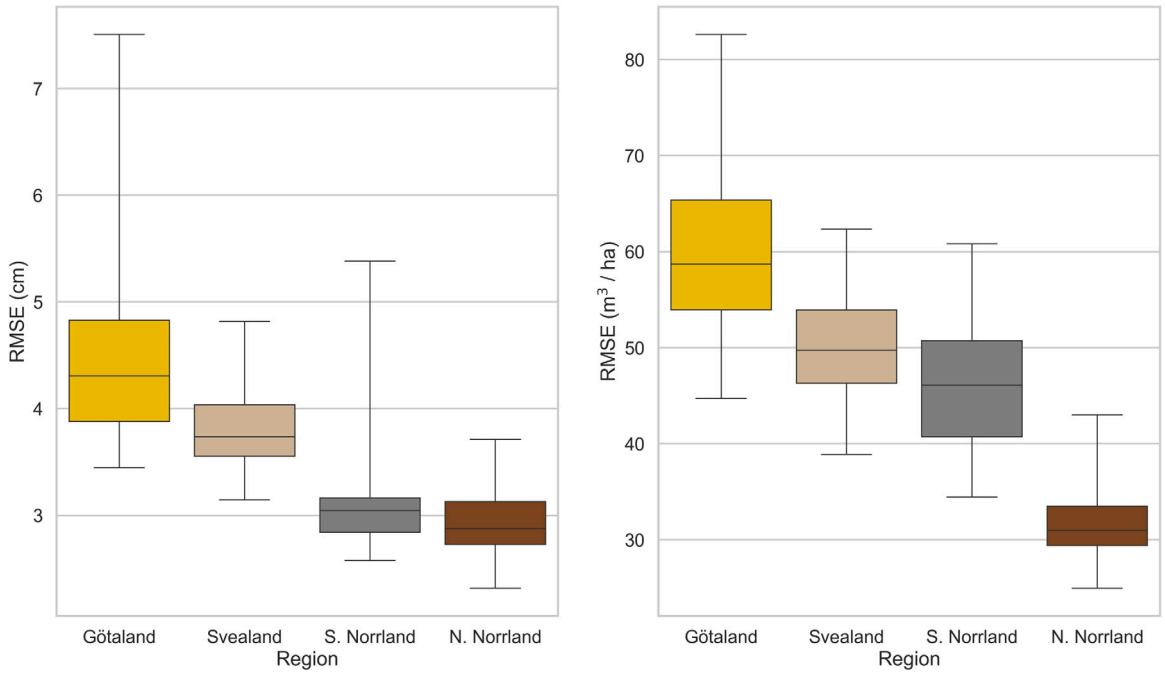

Fig. 8. Boxplots summarizing region-wise RMSE values over basal-area weighted mean stem diameter (left) and stem volume (right) predictions across 50 experiments. The RMSE values are obtained with the CNN model, but a similar trend can be observed with the other approaches as well.

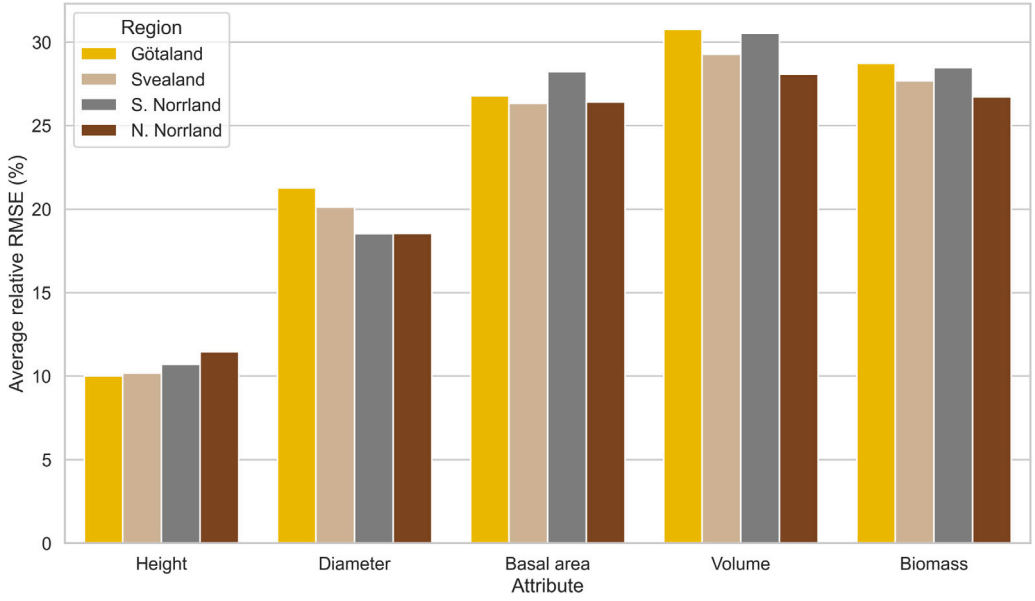

Fig. 9. Region-wise average relative RMSE values across 50 experiments over the forest attribute predictions. The relative RMSE estimates are obtained with the CNN model.

attribute predictions in Sweden, with the CNN specifically employed to investigate whether incorporating surrounding, correlated data further improves these predictions. ALS data were aggregated into 60 metrics, either clipped to the extent of the corresponding NFI plots or summarized in raster-like neighborhoods of 90 m × 90 m. XGBoost was trained using plot-level ALS metrics, while the CNN was provided with both the explicit plot-level ALS metrics and the surrounding raster information.

We found that the ML approaches outperformed the baseline linear regression models. In particular, predictions of diameter, basal area, and biomass improved when including surrounding ALS data and using a CNN, compared to using XGBoost on plot-level ALS metrics solely. This pattern was confirmed by the sensitivity analysis: even when progressively filtering up to 20% of potential outliers, the improvements from including surrounding information remained consistent, indicating that the additional ALS metrics possess meaningful predictive capacity and that the results are robust across various degrees of potential outliers.

The improvements for diameter, basal area, and biomass predictions may reflect the close relationships among these variables. Basal area is derived from DBH, and biomass is strongly associated with DBH, with many allometric equations using DBH as the sole predictor (Zianis and Mencuccini, 2004; Zianis et al., 2005). This is also consistent with Swedish practice, where biomass is estimated using Marklund's allometric functions, applying height-based equations only to trees in the

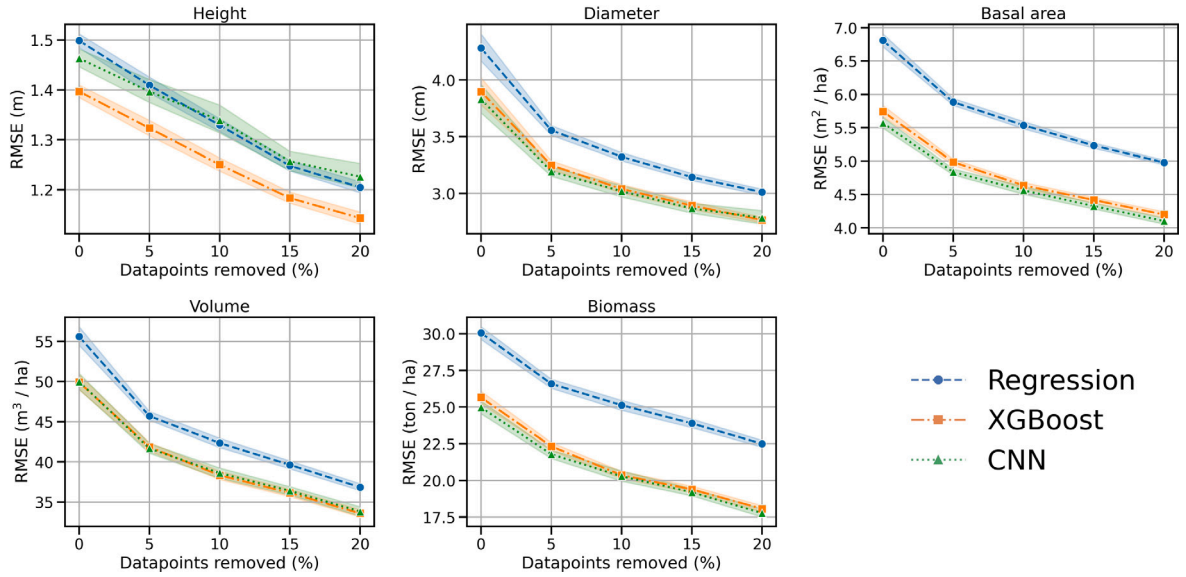

Fig. 10. Average RMSE values with 95% confidence intervals over the five different datasets used in the sensitivity analysis. The results are presented for all of Sweden.

Table 4
Hypothesis tests of model performance using the paired t-test and Wilcoxon signed rank test. Columns show whether RMSE differences were statistically significant. As both tests produced the same significance results, the statistical significance is summarized in one column.

Variable	Best ML vs. Baseline[a]	CNN vs. XGBoost[b]
Height	*	ns
Diameter	*	*
Basal area	*	*
Volume	*	ns
Biomass	*	*

ns: Not significant;
* $p < 0.05$.
[a] Alternative hypothesis: H_A: $\text{RMSE}_{\text{Best ML}} < \text{RMSE}_{\text{Baseline}}$.
[b] Alternative hypothesis: H_A: $\text{RMSE}_{\text{CNN}} < \text{RMSE}_{\text{XGBoost}}$.

height-measured subsample and DBH-only equations otherwise (Marklund, 1988; Nilsson et al., 2025). Therefore, it is reasonable that the predictions for diameter, basal area, and biomass show similar tendencies.

Including surrounding ALS data did not benefit height predictions. The CNN produced results similar to the linear regression model, and was outperformed by XGBoost. Tree height is already captured accurately by ALS measurements, so additional spatial context may not provide useful information and may instead introduce noise, reducing model performance.

Similarly, we found no evidence that including surrounding ALS data improves volume predictions, as the CNN yielded results comparable to those obtained using XGBoost. For trees in the height-measured subsample, volume is estimated using Näslund's function with DBH and height as inputs. For the remaining trees, form height is modeled using a set of predictors including tree species, DBH, basal area, altitude, latitude, stand age, site index, and mean height, after which volume is calculated using the DBH and the predicted form height (Åkesson and Westerlund, 2014). Because volume estimates rely on both DBH and height, the observed performance is consistent with the variable-specific results. Height prediction performance declined when including surrounding information, while predictions of diameter and basal area improved. Therefore, it is plausible that the volume predictions benefited from the improved DBH signal but were constrained by the degraded height component. Although biomass also depends on height, its relationship with DBH is much stronger than that of volume. Consequently, improvements in DBH predictions translate directly into better biomass estimates, whereas volume predictions are constrained by changes in both DBH and height.

These variable-specific results suggest that the effectiveness of including surrounding ALS data depends on the forest attribute. Research on spatial autocorrelation among forest attributes in Sweden would be recommended to further investigate these findings. In this context, such investigations can be used for determining optimal variable-specific neighborhood sizes to be used as inputs for ML models.

ML techniques offer flexible modeling approaches that can adapt to changing conditions and cross-country variation, making them well-suited for recalibration as new data become available, both within and across regions (Görgens et al., 2015). Our results directly support this advantage: no manual feature engineering was required, as the models learned from the full feature space and still achieved clear performance gains over the baseline linear regression models. These findings indicate that ML approaches are well-suited for large-scale and potentially cross-regional forest attribute mapping.

Based on our findings, several specific improvements could be considered for future national forest attribute mapping efforts. First, ML models, particularly CNNs, can incorporate spatial context to improve predictions of diameter, basal area, and biomass, suggesting that neighborhood information should be considered. Second, the flexibility of ML approaches allows them to handle large feature spaces without manual feature engineering, supporting easier recalibration as new ALS or NFI data become available.

In addition to these improvements, future work could explore even more advanced modeling strategies, such as voxelized representations of the point cloud (Balazs et al., 2022) or direct learning from raw point-cloud data (Chen et al., 2021). As future national ALS campaigns will be conducted using denser point clouds, these methods will become increasingly relevant, as demonstrated in Balazs et al. (2025). Moreover, because national ALS campaigns are typically conducted on 5–10 year cycles, the higher computational costs of these methods are less of a concern, as there is sufficient time for model training and inference within each cycle.

Compared to linear regression models, ML approaches (particularly the CNN in our case) are often regarded as "black boxes", making their interpretability challenging. To increase model interpretability, future work could investigate explainable artificial intelligence (XAI) (Xu

et al., 2019) techniques or hybrid modeling strategies to provide deeper insights into the model behavior and decision-making processes.

Additional input, such as data sources derived from aerial imagery or Sentinel-2, can also be merged with the modeling, which might improve the predictive capacity. For example, in Zhu and Liu (2015), NDVI time series data were used for above-ground biomass estimation. In Astola et al. (2019), a comparative study between Sentinel-2 and Landsat 8 imagery for forest attribute prediction was performed. The incorporation of these datasets can be used to attempt to improve the forest attribute predictions, but also to extend the predictions to a broader range of variables, such as tree species composition, which is also available in the Swedish NFI data.

6. Conclusion

In this work, ML approaches for prediction of forest attributes in Sweden were investigated. In particular, two ML approaches were tested: XGBoost and a CNN, where the CNN was used to test whether including surrounding ALS data was beneficial. We compare the results of our proposed ML models with baseline linear regression models, showcasing statistically significant improvements in the predictive accuracy of all five forest attributes, namely basal-area weighted mean tree height, basal-area weighted mean stem diameter, basal area, stem volume, and above-ground biomass. Moreover, small but statistically significant improvements for diameter, basal area, and above ground biomass predictions were observed by including surrounding ALS data and leveraging a CNN modeling approach. The results thus demonstrate the benefits of using ML models for creating national forest attribute maps. Consequently, the models developed in this work will be transferred for national forest attribute predictions in more countries, starting with Latvia. Including additional data sources such as Sentinel-2 will also be examined during the next phase of the project.

CRediT authorship contribution statement

Dag Björnberg: Writing – original draft, Visualization, Validation, Software, Methodology, Investigation, Formal analysis, Data curation, Conceptualization. **Morgan Ericsson:** Writing – review & editing, Supervision, Methodology, Conceptualization. **Johan Lindeberg:** Writing – review & editing, Supervision, Methodology, Conceptualization. **Welf Löwe:** Writing – review & editing, Supervision, Methodology, Conceptualization. **Jonas Nordqvist:** Writing – review & editing, Supervision, Methodology, Conceptualization. **Jörgen Wallerman:** Supervision, Methodology, Data curation, Conceptualization. **Johan E.S. Fransson:** Writing – review & editing, Supervision, Project administration, Methodology, Funding acquisition, Conceptualization.

Funding sources

This work was part of the ForestMap project which is supported under the umbrella of ERA-NET Cofund ForestValue by Swedish Governmental Agency for Innovation Systems, The Swedish Energy Agency, The Swedish Research Council for Environment, Agricultural Sciences and Spatial Planning, Academy of Finland, and The Scientific and Technological Research Council of Turkey. ForestValue has received funding from the European Union's Horizon 2020 research and innovation programme under grant agreement No. 773324. Dag Björnberg's work was (in addition to ForestMap) funded by the Industry Graduate School on "Data Intensive Applications (DIA)" at Linnæus University which is partially funded by The Knowledge Foundation, Sweden (project id 20190336).

Declaration of competing interest

The authors declare that they have no known competing financial interests or personal relationships that could have appeared to influence the work reported in this paper.

Acknowledgments

The authors would like to thank the co-members of the ForestMap project Shafiullah Somroo and Jorge Lazo, for great collaboration and interesting talks.

Data availability

ALS point cloud data are freely available through Lantmäteriet. A sample of temporary plot data collected between 2007 and 2023 is available via the Swedish University of Agricultural Sciences (SLU). Data from permanent plots inventoried since 1983 can be ordered but are as of now, not publicly available. Exact coordinates of permanent plots are unavailable, as releasing these compromises data integrity. Consequently, the coordinates for such plots (if downloaded) have an offset, and can therefore not directly be used in combination with ALS data from Lantmäteriet. For researchers, a confidentiality agreement can be discussed to obtain access to the exact coordinates. Contact SLU for more information.

References

Aggarwal, C.C., 2018. Convolutional neural networks. In: Neural Networks and Deep Learning: A Textbook. Springer International Publishing, Cham, pp. 315–371.

Åkesson, H., Westerlund, B., 2014. Konstruktion, Test Och Underhåll av Simuleringsfunktioner i Riksskogstaxeringen. Arbetsrapport/Sveriges lantbruksuniversitet, Institutionen för skoglig resurshushållning, (419).

Astola, H., Häme, T., Sirro, L., Molinier, M., Kilpi, J., 2019. Comparison of Sentinel-2 and Landsat 8 imagery for forest variable prediction in boreal region. Remote Sens. Environ. 223, 257–273.

Balazs, A., Liski, E., Tuominen, S., Kangas, A., 2022. Comparison of neural networks and k-nearest neighbors methods in forest stand variable estimation using airborne laser data. ISPRS Open J. Photogramm. Remote Sens. 4, 100012.

Balazs, A., Tuominen, S., Kangas, A., 2025. Enhancing forest inventory Accuracy: Comparing 3D-CNN and k-NN with genetic algorithm Approaches using ALS data across boreal bioregions. Comput. Electron. Agric. 237, 110576.

Baldi, P., Sadowski, P.J., 2013. Understanding dropout. Adv. Neural Inf. Process. Syst. 26.

Bengio, Y., Courville, A., Vincent, P., 2013. Representation learning: A review and new perspectives. IEEE Trans. Pattern Anal. Mach. Intell. 35 (8), 1798–1828.

Chen, T., Guestrin, C., 2016. Xgboost: A scalable tree boosting system. In: Proceedings of the 22nd Acm Sigkdd International Conference on Knowledge Discovery and Data Mining. pp. 785–794.

Chen, X., Jiang, K., Zhu, Y., Wang, X., Yun, T., 2021. Individual tree crown segmentation directly from UAV-borne LiDAR data using the PointNet of deep learning. Forests 12 (2), 131.

Dash, J., Pont, D., Brownlie, R., Dunningham, A., Watt, M., Pearse, G., 2016. Remote sensing for precision forestry. NZJ For. 60 (4), 15–24.

de Lera Garrido, A., Gobakken, T., Hauglin, M., Næsset, E., Bollandsås, O.M., 2023. Accuracy assessment of the nationwide forest attribute map of Norway constructed by using airborne laser scanning data and field data from the national forest inventory. Scand. J. For. Res. 38 (1–2), 9–22.

De Maesschalck, R., Jouan-Rimbaud, D., Massart, D.L., 2000. The mahalanobis distance. Chemometr. Intell. Lab. Syst. 50 (1), 1–18.

Domingos, P., 2012. A few useful things to know about machine learning. Commun. ACM 55 (10), 78–87.

Elfving, B., Nyström, K., 2010. Growth Modelling in the Heureka System. Department of Forest Ecology and Management, Swedish University of Agricultural Sciences, Umeå, Sweden, p. 97.

Eliasson, L., Manner, J., Thor, M., 2019. Costs for thinning and final felling operations in Sweden, 2000–2017. Scand. J. For. Res. 34 (7), 627–634.

Fahlvik, N., Elfving, B., Wikström, P., 2014. Evaluation of growth functions used in the Swedish Forest Planning System Heureka. Silva Fenn. 48 (2).

Fridman, J., Holm, S., Nilsson, M., Nilsson, P., Ringvall, A.H., Ståhl, G., 2014. Adapting National Forest Inventories to changing requirements–the case of the Swedish National Forest Inventory at the turn of the 20th century. Silva Fenn. 48 (3).

Friedman, J.H., 2001. Greedy function approximation: a gradient boosting machine. Ann. Stat. 1189–1232.

Görgens, E.B., Montaghi, A., Rodriguez, L.C.E., 2015. A performance comparison of machine learning methods to estimate the fast-growing forest plantation yield based on laser scanning metrics. Comput. Electron. Agric. 116, 221–227.

Grinsztajn, L., Oyallon, E., Varoquaux, G., 2022. Why do tree-based models still outperform deep learning on typical tabular data? Adv. Neural Inf. Process. Syst. 35, 507–520.

Janiec, P., Tymińska-Czabańska, L., Hawryło, P., Woda, M., Socha, J., 2025. Determining vertical structure of forests in Poland using a semi-automated approach based on ALS data. Ecol. Indic. 178, 113825.

Kattenborn, T., Leitloff, J., Schiefer, F., Hinz, S., 2021. Review on Convolutional Neural Networks (CNN) in vegetation remote sensing. ISPRS J. Photogramm. Remote Sens. 173, 24–49.

Knott, J.A., Liknes, G.C., Giebink, C.L., Oh, S., Domke, G.M., McRoberts, R.E., Quirino, V.F., Walters, B.F., 2023. Effects of outliers on remote sensing-assisted forest biomass estimation: A case study from the United States national forest inventory. Methods Ecol. Evol. 14 (7), 1587–1602.

Lee, J., Im, J., Kim, K., Quackenbush, L.J., 2018. Machine learning approaches for estimating forest stand height using plot-based observations and airborne LiDAR data. Forests 9 (5), 268.

Maltamo, M., Kinnunen, H., Kangas, A., Korhonen, L., 2020. Predicting stand age in managed forests using National Forest Inventory field data and airborne laser scanning. For. Ecosyst. 7, 1–11.

Maltamo, M., Packalen, P., Kangas, A., 2021. From comprehensive field inventories to remotely sensed wall-to-wall stand attribute data—a brief history of management inventories in the Nordic countries. Can. J. Forest Res. 51 (2), 257–266.

Marklund, L., 1988. Biomassafunktioner för Tall, Gran Och Björk i Sverige. In: Rapport: Institutionen för Skogstaxering, Institutionen för skogstaxering, Sveriges lantbruksuniversitet.

Næsset, E., 2002. Predicting forest stand characteristics with airborne scanning laser using a practical two-stage procedure and field data. Remote Sens. Environ. 80 (1), 88–99.

Næsset, E., Gobakken, T., Holmgren, J., Hyyppä, H., Hyyppä, J., Maltamo, M., Nilsson, M., Olsson, H., Persson, Å., Söderman, U., 2004. Laser scanning of forest resources: the Nordic experience. Scand. J. For. Res. 19 (6), 482–499.

Nilsson, P., Markström, M., Fridman, J., 2025. Skogsdata 2025. Skogsdata (2025).

Nilsson, M., Nordkvist, K., Jonzén, J., Lindgren, N., Axensten, P., Wallerman, J., Egberth, M., Larsson, S., Nilsson, L., Eriksson, J., et al., 2017. A nationwide forest attribute map of Sweden predicted using airborne laser scanning data and field data from the National Forest Inventory. Remote Sens. Environ. 194, 447–454.

Nord-Larsen, T., Schumacher, J., 2012. Estimation of forest resources from a country wide laser scanning survey and national forest inventory data. Remote Sens. Environ. 119, 148–157.

Parkitna, K., Krok, G., Miścicki, S., Ukalski, K., Lisańczuk, M., Mitelsztedt, K., Magnussen, S., Markiewicz, A., Stereńczak, K., 2021. Modelling growing stock volume of forest stands with various ALS area-based approaches. For.: Int. J. For. Res. 94 (5), 630–650.

Persson, H.J., Olsson, H., Soja, M.J., Ulander, L.M., Fransson, J.E., 2017. Experiences from large-scale forest mapping of Sweden using TanDEM-X data. Remote Sens. 9 (12), 1253.

Ranneby, B., Cruse, T., Hägglund, B., Jonasson, H., Swärd, J., 1987. Designing a New National Forest Survey for Sweden.

Rosner, B., 1983. Percentage points for a generalized ESD many-outlier procedure. Technometrics 25 (2), 165–172.

Roussel, J.-R., Auty, D., Coops, N.C., Tompalski, P., Goodbody, T.R., Meador, A.S., Bourdon, J.-F., De Boissieu, F., Achim, A., 2020. lidR: An R package for analysis of Airborne Laser Scanning (ALS) data. Remote Sens. Environ. 251, 112061.

Seabold, S., Perktold, J., et al., 2010. Statsmodels: econometric and statistical modeling with python. SciPy 7 (1), 92–96.

Tuominen, S., Pitkänen, T., Balazs, A., Kangas, A., 2017. Improving Finnish multi-source national forest inventory by 3D aerial imaging. Silva Fenn. 51 (4).

Valbuena, R., Maltamo, M., Mehtätalo, L., Packalen, P., 2017. Key structural features of Boreal forests may be detected directly using L-moments from airborne lidar data. Remote Sens. Environ. 194, 437–446.

Vijaywargiya, J., Ramiya, A.M., 2024. Semantic segmentation of urban airborne LiDAR data of varying landcover diversity using XGBoost. IET Comput. Vis..

Wen, L., Gao, L., Li, X., Zeng, B., 2021. Convolutional neural network with automatic learning rate scheduler for fault classification. IEEE Trans. Instrum. Meas. 70, 1–12.

Xu, F., Uszkoreit, H., Du, Y., Fan, W., Zhao, D., Zhu, J., 2019. Explainable AI: A brief survey on history, research areas, approaches and challenges. In: CCF International Conference on Natural Language Processing and Chinese Computing. Springer, pp. 563–574.

Zamani Joharestani, M., Cao, C., Ni, X., Bashir, B., Talebiesfandarani, S., 2019. PM2. 5 prediction based on random forest, XGBoost, and deep learning using multisource remote sensing data. Atmosphere 10 (7), 373.

Zhang, X., Chen, G., Liu, C., Fan, Q., Li, W., Wu, Y., Xu, H., Ou, G., 2023. Spatial effects analysis on individual-tree aboveground biomass in a tropical Pinus kesiya var. langbianensis natural forest in Yunnan, Southwestern China. Forests 14 (6), 1177.

Zhu, X., Liu, D., 2015. Improving forest aboveground biomass estimation using seasonal Landsat NDVI time-series. ISPRS J. Photogramm. Remote Sens. 102, 222–231.

Zianis, D., Mencuccini, M., 2004. On simplifying allometric analyses of forest biomass. Forest Ecol. Manag. 187 (2–3), 311–332.

Zianis, D., Muukkonen, P., Mäkipää, R., Mencuccini, M., 2005. Biomass and Stem Volume Equations for Tree Species in Europe.